UDC 532.54

HYDRODYNAMICS OF HYDROCYCLONE WITH BUILT-IN WATER INJECTOR

[1]L. Minkov, [2]M. Farghaly, [3]J. Dueck

[1]Tomsk State University, Tomsk, Russia

[2]Al-azhar University, Egypt

[3]Friedrich-Alexander-University, Erlangen-Nuremberg, Germany, lminkov@ftf.tsu.ru

The paper considers the numerical simulation of 3D fluid dynamics based on the k-eps RNG model of turbulence in the hydrocyclone with the injector, containing 5 tangentially directed nozzles. The simulation results are supported by experimental research. It is shown that the direction of movement of injected fluid in the hydrocyclone depends on the water flow rate through the injector. Experiments and calculations show that the dependence of the Split-parameter on the injected water flow rate has a non-monotone character associated with the ratio of power of the main flow and the injected fluid.

Keywords: numerical simulation, hydrocyclone, injector, injected fluid, water flow rate, split-parameter.

Introduction

The basic separation principle employed in hydrocyclones, which are widely used in different fields of engineering applications, is the centrifugal sedimentation. Feed slurry is introduced under pressure via the tangential inlet and is constrained by the geometry of the unit to move into a circular path. This creates the outward centrifugal force and the convective flux of particles toward the wall.

In spite of its simple configuration, the hydrocyclone has a complex flow field. The characteristics of the hydrocyclone flow are as follows: very strong circulation, complex turbulent fields, formation of closed circulation zones, and formation of the air core near the central axis zone.

Turbulent diffusion prevents fine particles to accumulate near the wall of hydrocyclone and even leads to make them spreads over the whole space of the hydrocyclone. In case of neglecting the influence of the centrifugal force on the fine particles, they will leave the hydrocyclone proportionally to the quantities of water flowing out through both outlets.

Many researchers [1-9] were interesting to study the hydrocyclone hydrodynamics (computational mathematics) that theoretically and experimentally revealed basic characteristic features of hydrocyclone flow while other studies were focusing on the technological aspects of the solid-liquid separation or size classification [10 – 15].

The typical disadvantages of hydrocyclone operation can be summarized as follows: incomplete separation of solid phase especially the fine fractions, insufficient quality of the separation, and the relatively small value of cut size. These disadvantages can be partially eliminated by changing the design parameters of the hydrocyclone or by variation of the hydrocyclone feed pressure. Changing the hydrocyclone configuration to improve the separation and classification processes have been undertaken for a sufficiently long time.

One of these techniques is the water injection into the conical part of the hydrocyclone [16 – 21]. Recently, a new water injection hydrocyclone which is characterized by the injection in the lowest possible position near the hydrocyclone apex is developed and is schematically shown in Fig.1. A simplified mathematical model of classification in a hydrocyclone is presented in [22]. Further development requires a deep knowledge of hydrodynamics in the hydrocyclone with the injector.

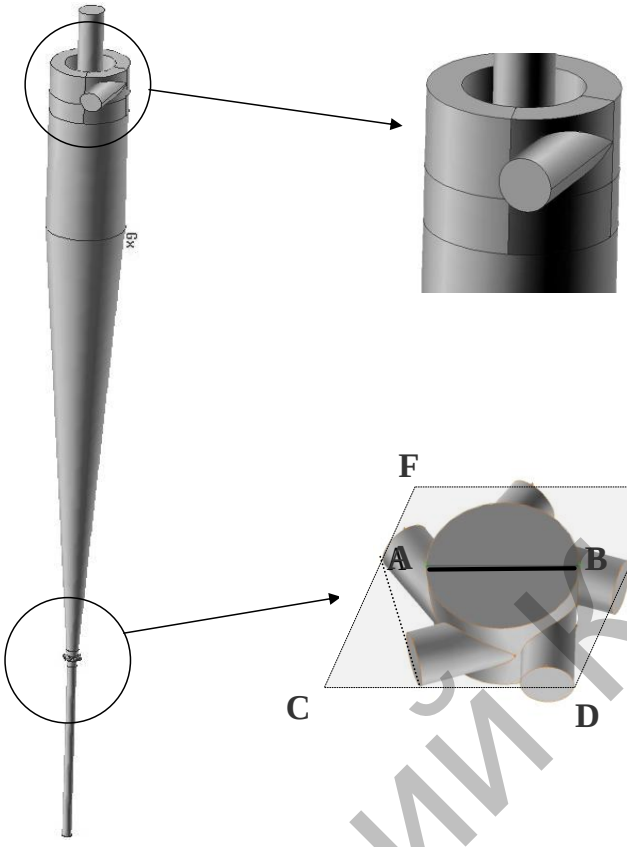

Fig. 1. Scheme of hydrocyclone and water injector

Water injection is expected to wash out the fine particles from the wall boundary layer to the axis where particles are swept up by upward flow and then discharge through the overflow. Accordingly, fine particles missreported through the underflow discharge will be decreased .

The effect of the injection depends on many parameters such as; the amount of injected water, the injection velocity, the position of injection and many other parameterswhich should be optimised. Besides the experimental investigations, the modelling processes of the injection is of great importance to describe the injection mechanism. Models describing the influence of water injection on the separation efficiency of dispersed material have found not enough in the literature till now. Such models could be created on the base of appropriated investigations of the hydrodynamics but, the hydromechanics of flow in case of water injection hydrocyclone is not described in the literature.

Modeling the hydrodynamics in hydrocyclone with water injector supported by experiments is the aim of this work. Special emphasis were focused on to explain the mechanism of injection and its influence on the variation of fluid flow field, and hence on the classification mechanisms.

Experimental test rig and procedures

The test-rig used in the experimental work consisted of a 50-mm water injection cyclone positioned vertically above a feed tank (Fig. 2).

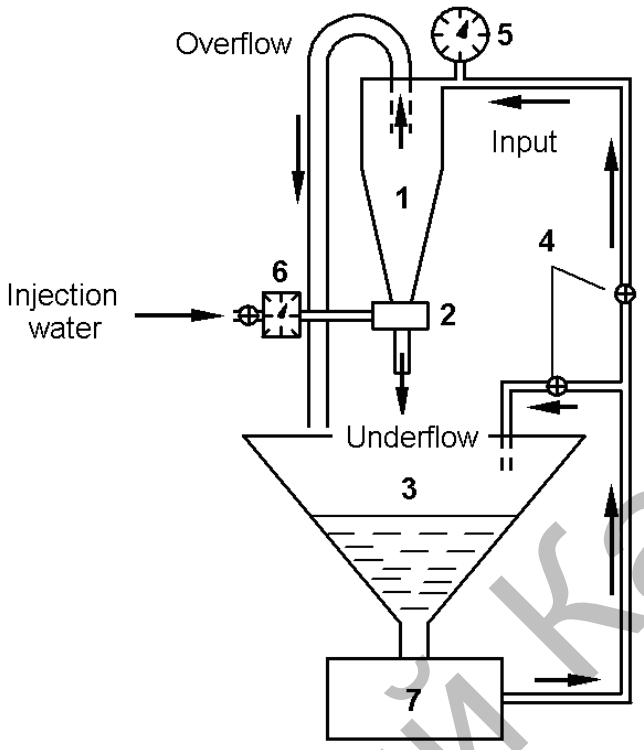

Fig. 2. Water injection hydrocyclone test rig. 1 – Water injection cyclone, 2 – Injector, 3 – Feed slurry tank, 4 – Control valves, 5 – Pressure gauge, 6 – Manometer, 7 – Pump.

The outlet of the pump is connected to the hydrocyclone feed inlet. A by-pass pipe with a control valve was connected to the outlet line to obtain the desired pressure drop inside the cyclone. A pressure gauge was fitted near the feed inlet to indicate the pressure drop. The water injection cyclone which is used through this work is a conventional hydrocyclone with a modified conical part with water injection facility.

The water injection assembly consists of an outer solid ring and inner solid ring with 5 inlet openings at equal distances opened directly on the periphery of the cone part as shown in Fig. 1. This assembly is connected with water control valve through which the water can be supplied under pressure in the assembly and injected through these openings. A digital flowmeter was fixed near the water injection to indicate the water injection rate.

The injection ring was designed to permit the water to be injected in a tangential direction with the same swirling direction as the main flow inside the hydrocyclone. The ring when attaches to the cone part will have the same internal geometry of it without any mechanical parts to be inserted inside the cone part to avoid any mechanical disturbing of the flow inside the hydrocyclone. The water injection part was added near the apex of the cyclone without causing any extension of the total cyclone length.

A pre-selected vortex finder and apex were fitted to the body of the water injection cyclone and then the feed is pumped at the required inlet pressure. The steady state is reached through nearly one minute.

To investigate the effect of water injection rate on the hydrodynamics of the separation, samples were taken at different flow rates of injection. From these samples, the feed flow rate, overflow rate, and underflow rate can be calculated at every test from which the split - parameter can be estimated.

Numerical model

The geometry of the hydrocyclone is given in Fig. 3. The grid for a discrete description of flow field was realized with the help of a computer software (Gambit 2.3.16., Fluent Inc. ©) to create the 3D body fitted grid of 170000 cells. Calculation of hydrodynamics was done on the base of Fluent 6.3.26 software.

The set of Navier-Stokes equations includes:

Continuity equation $\frac{\partial u_i}{\partial x_i} = 0$, $i = 1,2,3$

Momentum equation $\frac{\partial u_i u_j}{\partial x_j} + \frac{\partial p}{\partial x_i} = \frac{\partial}{\partial x_j}\left(\mu_{eff}\frac{\partial u_i}{\partial x_j}\right)$, $i, j = 1,2,3$

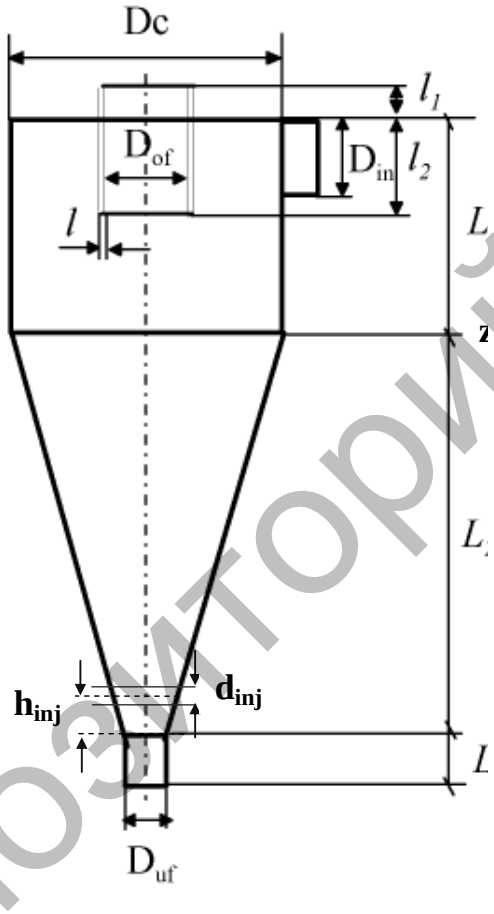

D_c	50 mm
D_{in}	14.5 mm
D_o	16 mm
D_u	6 mm
L_1	130 mm
L_2	350 mm
L_3	135 mm
$l_1 + l_2$	79 mm
l_2	37 mm
l	8 mm
d_{inj}	2.5 mm
h_{inj}	20 mm

Fig. 3. Geometry of water injection hydrocyclone

The RNG $k-\varepsilon$ model of turbulence [23] is used to calculate effective viscosity $\mu_{eff} = \mu_{mol} + \mu_t$

– The turbulence kinetic energy equation $\frac{\partial \rho k u_i}{\partial x_i} = \frac{\partial}{\partial x_j}\left(\alpha_k \mu_{eff}\frac{\partial k}{\partial x_j}\right) + G_k - \rho\varepsilon$

– The dissipation rate of turbulence kinetic energy equation

$$\frac{\partial \rho \varepsilon u_i}{\partial x_i} = \frac{\partial}{\partial x_j}\left(\alpha_\varepsilon \mu_{eff}\frac{\partial \varepsilon}{\partial x_j}\right) + \frac{\varepsilon}{k}\left(C_{1\varepsilon}G_k - C_{2\varepsilon}\rho\varepsilon\right)$$

Knowing values of the turbulence kinetic energy and its dissipation rate one can calculate the value of turbulent viscosity as follows:

$$\mu_t = \rho C_\mu \frac{k^2}{\varepsilon} f\left(\alpha_s, \Omega, \frac{k}{\varepsilon}\right),$$

Where: $f\left(\alpha_s, \Omega, \frac{k}{\varepsilon}\right)$ = the correction function taking into account a swirling flow [FLUENT 6.3 User's Guide. Fluent Inc. 2006-09-20.- 2006].

$$G_k = \mu_t S^2; \qquad S \equiv \sqrt{2 S_{ij} S_{ij}}$$

Where:

S_{ij} = mean rate-of-strain tensor $= \frac{1}{2}\left(\frac{\partial u_j}{\partial x_i} + \frac{\partial u_i}{\partial x_j}\right)$; $C_{2\varepsilon} = C_2 + \frac{C_\mu \eta^3 (1 - \eta/\eta_0)}{1 + \beta \eta^3}$

Where: $\eta \equiv S \frac{k}{\varepsilon}$

Model constants:

$\alpha_k = \alpha_\varepsilon \approx 1.393$; $\alpha_s = 0.15$; $\beta = 0.012$; $C_{1\varepsilon} = 1.42$; $C_\mu = 0.0845$; $\eta_0 = 4.38$.

Boundary conditions:

a) At the inlet of main feed pipe.

Normal component of inlet velocity: $u_n = \frac{4Q_{inlet}}{\pi D_{inlet}^2}$

Tangent component of inlet velocity: $u_\tau = 0$

Turbulence kinetic energy: $k = \frac{3}{2} 10^{-2} (u_n)^2$

Dissipation rate of turbulence kinetic energy: $\varepsilon = C_\mu^{3/4} \frac{k^{3/2}}{0.07 D_{inlet}}$

Where:

D_{inlet} = diameter of feed pipe

Q_{inlet} = volumetric flow rate at the inlet of main feed pipe

b) At the inlet of injector feed pipe:

Normal component of injection velocity $u_n = \frac{4Q_{inj}}{\pi d_{inj}^2}$

Tangent component of inlet velocity $u_\tau = 0$

Turbulence kinetic energy $k = \frac{3}{2} 10^{-2} (u_n)^2$

Dissipation rate of turbulence kinetic energy $\varepsilon = C_\mu^{3/4} \frac{k^{3/2}}{0.07 d_{inj}}$

Where:

d_{inj} = diameter of injector pipe

Q_{inj} = volumetric flow rate at the inlet of injector pipe

c) On the injector and hydrocyclone walls:

No-slip conditions were chosen $u_i = 0$

d) At the outlets:

The ambient pressure was applied in the centre of the upper flow and underflow outlets and the condition of equilibrium of the centrifugal forces with the radial pressure gradient was used in the internal points of the outlets:

$$\frac{\partial p}{\partial r} = \frac{\rho u_\tau^2}{r}$$

The set of equations (1) - (4) was numerically solved using the upwind differential scheme of second order of accuracy for convective terms and the second order of accuracy for pressure gradients. SIMPLEC was used for the pressure-velocity coupling.

Results and Discussion

1 Stream lines and velocity fields

The flow field of fluid in the conical part of hydrocyclone on the section included the axis of cyclone and the straight line AB is showed in Fig. 1 above the injector and is depicted in Fig. 4 (y = 0, z = - 0.341 m). It should be noted, that using of 5 injectors tubes leads to asymmetrical profiles of velocities.

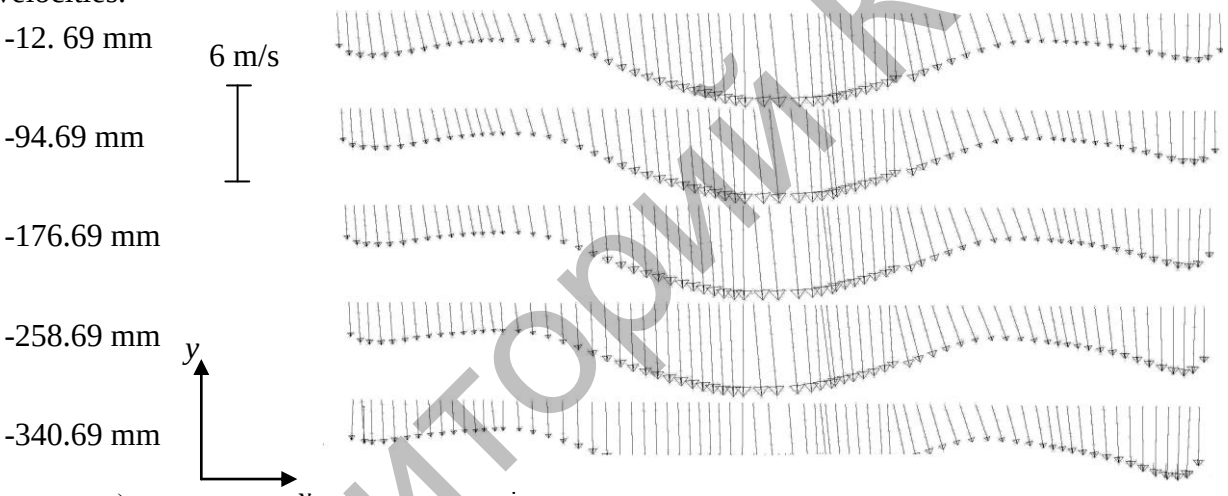

a)

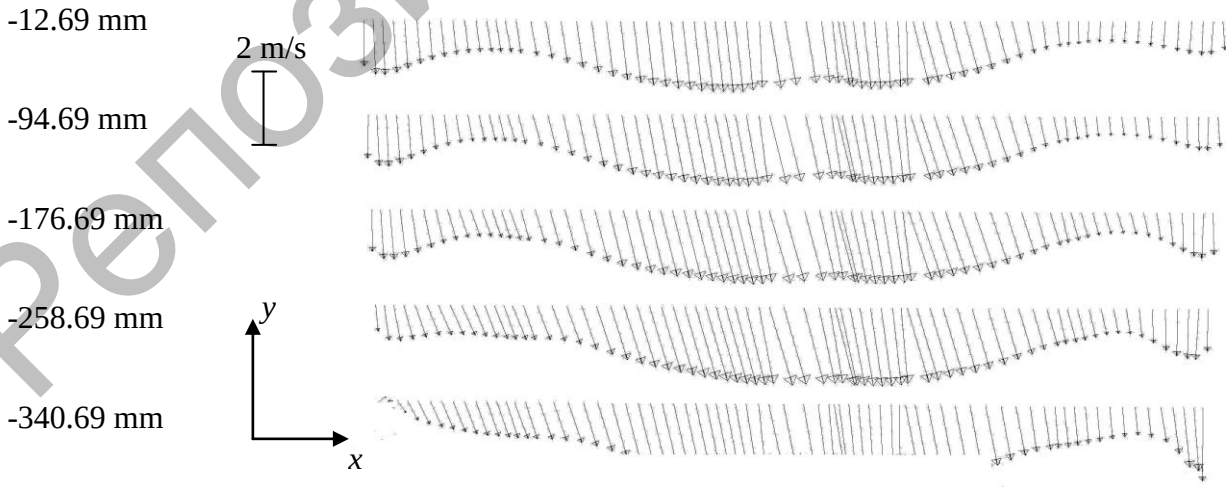

b)

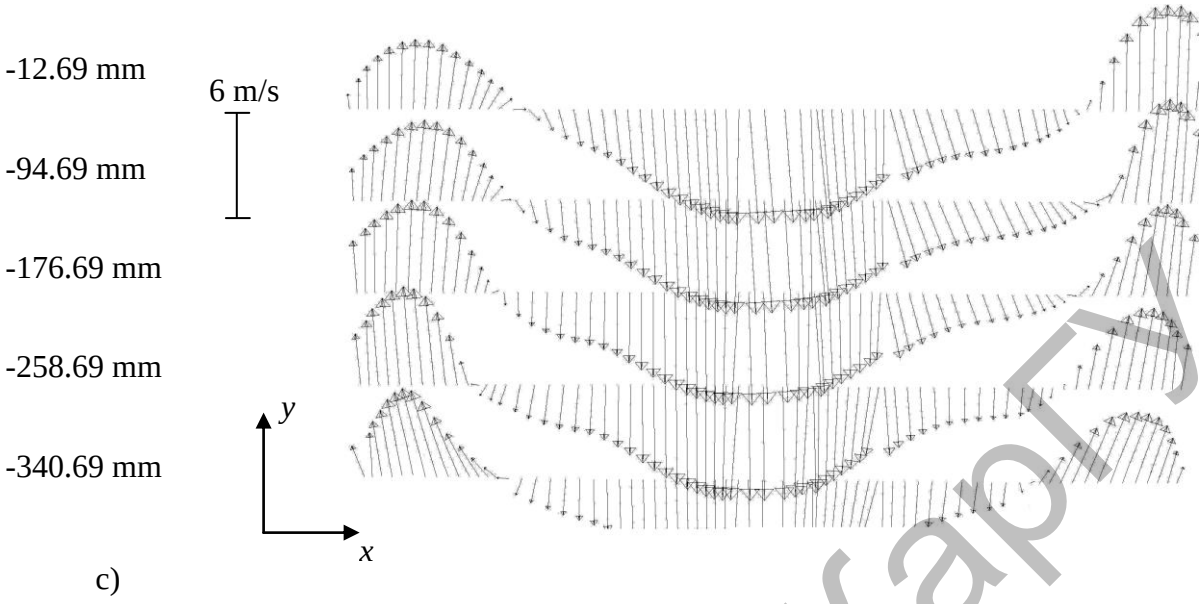

Fig. 4. Flow fields above the injector (z = - 0.341 m). Q_{feed}= 63.62 l/min a) Q_{inj}= 0 l/min; b) Q_{inj}= 4 l/min;, c) Q_{inj}= 9 l/min

In the calculations, and the subsequent presentation of the results a rectangular coordinate system was used. Coordinate x is measured along the line AB as shown in Fig. 1 and the coordinate z is measured along the axis of the hydrocyclone, beginning with the transition cross section of the cylindrical part of the hydrocyclone in a conical one, as shown in Fig. 1.

In case of no injection, the increased velocity zone directed to the apex takes place near the axial domain (Fig.4 a). The velocity profile at low values of injection rate (Q_{inj}= 4 lpm) becomes flat (Fig.4 b) whereas at high values of injection rate (Q_{inj}=9 lpm) the reorganization of flow field takes place near the wall of hydrocyclone, zones of flow inverse directed to the main one are formed (Fig.4 b). Similar conclusions can be made by analysis of Fig.5.

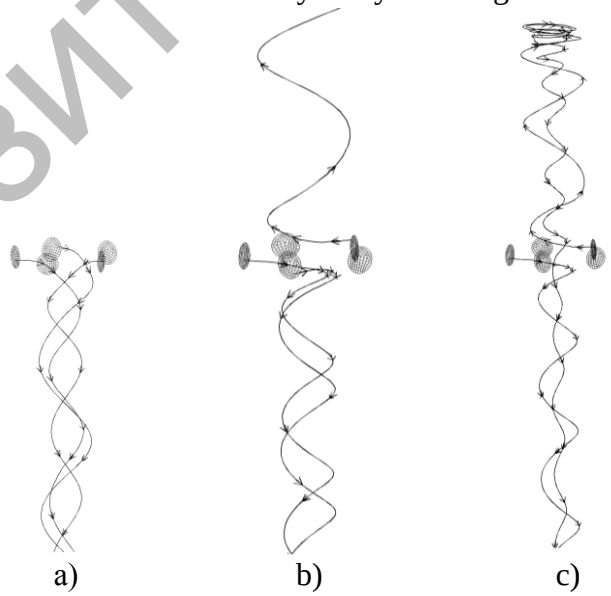

Fig. 5. Trajectories of fluid. Q_{feed}=63.62 l/min. a) Q_{inj}=0 l/min; b) Q_{inj}=4 l/min., c) Q_{inj}=9 l/min. 1 – Trajectory of fluid particle leaving the hydrocyclone through the upper outlet. 2 – Trajectory of fluid particle leaving the hydrocyclone through the down outlet.

Fig. 5 shows the swirling trajectories of the injected liquid for nonzero rates: 4 lpm, (Fig. 5 a) and 9 lpm, (Fig. 5 b and Fig. 5 c). At low injection rate (Q_{inj}= 4 lpm) most of the injected water is entrained by the main flow and leaves the hydrocyclone through the underflow which leads to the increasing the water discharge through the underflow.

At high injection rate (Q_{inj} = 9 lpm) in Fig. 5b one can see the trajectories of injected fluid are both upward and downward. This means that the injected liquid can be entrained by two streams and can be removed from the apparatus through the both outlets. It is interesting to note that at this injection intensity (Q_{inj} = 9 lpm) among trajectories initially directed upwards, there are those which at a certain height relative to the injector are fully turned and finish at the underflow apex (Fig. 5 c, trajectory 2).

2 Velocity components

The following results were picked up on the section included the axis of apparatus and the straight line AB, showed in Fig. 1. Along this line is the x-coordinate, which intersected with the axis of apparatus (axis of hydrocyclone).

2.1 Axial velocity

The profiles of the axial velocity are shown in Fig. 6. The axial velocity above the position of the injector is shown in Fig. 6a while the axial velocity under the position of the injector is shown in Fig. 6b. At low injection rate the power of injected water is small to overcome the resistance of the main flow. Additional resistance created by the injected water results in the stagnation of main flow near the injector. All flux from the injector directs to the underflow that leads to the increase in the axial velocity of flow into the apex.

At injection with flow rate equal to 4 lpm, all the liquid flowing through the inlet, leaves the hydrocyclone either through the overflow or through the underflow, while the injected liquid flows only through the underflow. When Q_{inj} = 9 lpm, the power of injected jet is enough to overcome the resistance of the main flow and the injected liquid flows both through the underflow and through the overflow while the liquid fed through the inlet flows through the underflow discharge.

At high injection rate the upward swirling flow along the wall of cone part of hydrocyclone is formed upstream. At the zone near the axis the downward swirl rotating co-axial with the outer vortex is developed.

The three minima presented in the velocity distribution in Fig. 6b can be explained by the presence of two whirls present in this part of the apparatus; one is formed on the periphery as a result of the liquid which comes directly from the injector to the apex, the other central whirl formed by a liquid which is carried away from the injector upwards which is braked as a result of interaction with the main downwards stream.

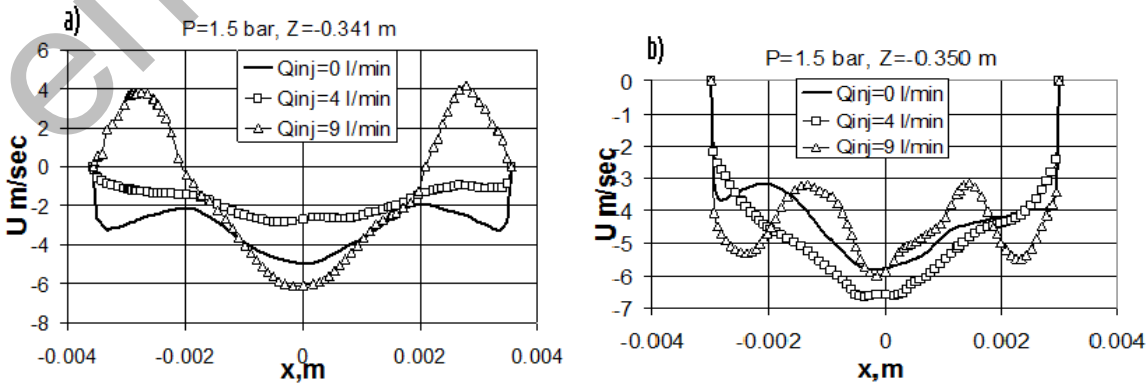

Fig. 6. Dependence of axial velocity distribution of a transverse coordinates x at various velocities of injected water Q_{inj}. a) Z=–0.341 m (above the injector position), b) Z= –0.350m (under the injectors position)

2.2 Tangential velocity

Fig. 7 shows the distribution of the tangential velocity. This velocity component, as a source of centrifugal force, affects critically the classification performance.

In Fig. 7 a mild injection leads to a reduction in the tangential velocity on the periphery of liquid (at 4 lpm). Increasing of the injected velocity leads to an increase in the tangential component of flow. Thus the tangential velocity increases in the whole flow (at 9 lpm). Near the axis zone the velocity distribution of rotating flow is similar to the velocity distribution of a solid body (profiles tangential velocities are close to straight lines). Towards the periphery, the velocities profiles change the sign of their second derivative, which showed, as stated previously, the existence of internal injector swirl rotating at a velocity different from the velocity of the external vortex.

Fig. 7b shows the tangential velocity profiles at the position under the injectors at different velocity of injected water. At low injection velocity of 4 lpm, only weak changes are occurred at the profile tangential speed below the injector, while at high injection speed of 9 lpm the velocity of the flow near the wall of apex is increased.

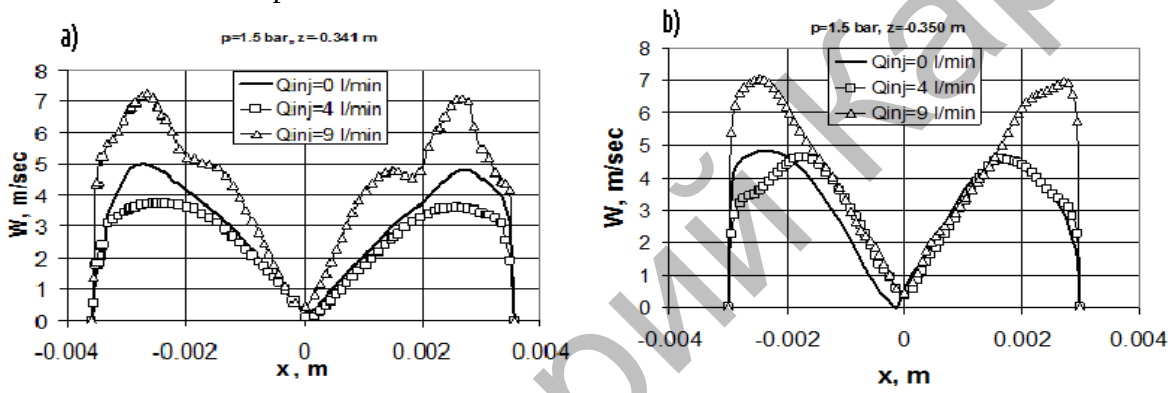

Fig. 7. Profiles of tangential velocity a) above the injector. (Z= –0.341 mm), b) below the injector. (Z= –0.350 mm).

2.3 Radial velocity

A strong restructuring of the profile of the radial velocity occurs above the injector (Fig. 8a).

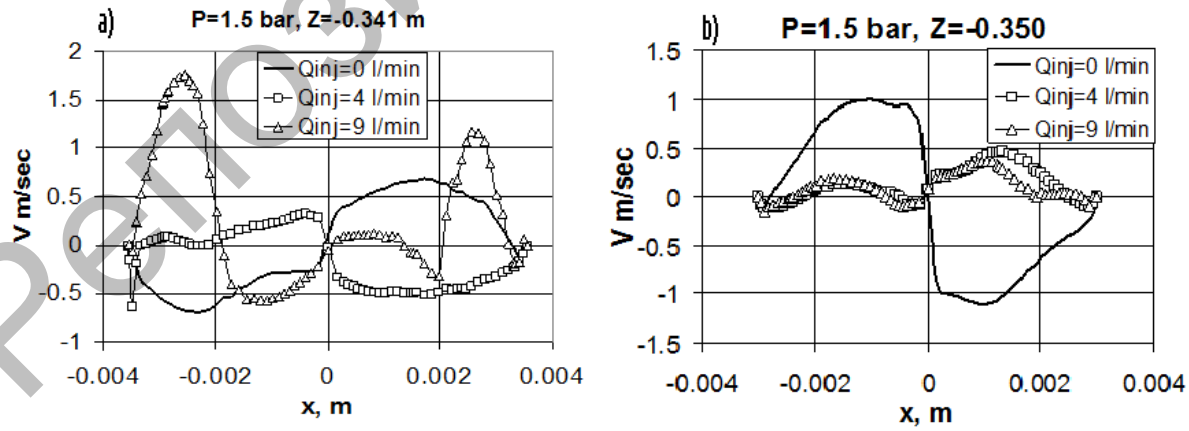

Fig. 8. Profiles of radial velocity a) over the injector (Z= –0.341 m), b) under the injector (Z= –0.350 m), Arrows indicate the direction of the radial velocity at 9.0 lpm

In case of no injection, the fluid is directed from the axis to the walls (solid curve at Q_{inj}=0).

The curves are rather symmetrical relatively to the z-axis. The positive values of radial velocity at x> 0 indicate the movement from the axis to the wall, as negative for x<0. The low injection

velocity reduces the radial velocity and changes its direction to the opposite from the periphery to the center (the curve at Q_{inj}=4 lpm). At high injection rates there is a non monotone and asymmetrical profile of radial velocity (curve at Q_{inj}=4 lpm). Near the axis the flow is directed to the periphery of the axis, while near to the walls the motion may be directed inward (the left part profile) and outside (the right side profile). Under the injector (Fig. 8b) the radial velocity is directed mostly to the wall. The radial velocity is rather weaker in comparison with the case without injection.

3 Pressure

Increasing the injected water generates upwards flow which forms additional hydraulic resistance. Consequently, the pressure in the inlet increases according to adjusted constant flow rate of water.

Fig. 9 shows the calculated increase in the pressure values at the feed inlet with increasing of the injected liquid velocity (under condition that the feed throughput is constant). This should be taken into account during the experiments. Such increase of pressure in the feed is observed during the experiments and requires readjusting the pressure, if a constant pressure is desired. The dependence of the pressure increase on the rate of injection is describing well by the power dependence with an exponent approximately equal to 1.3.

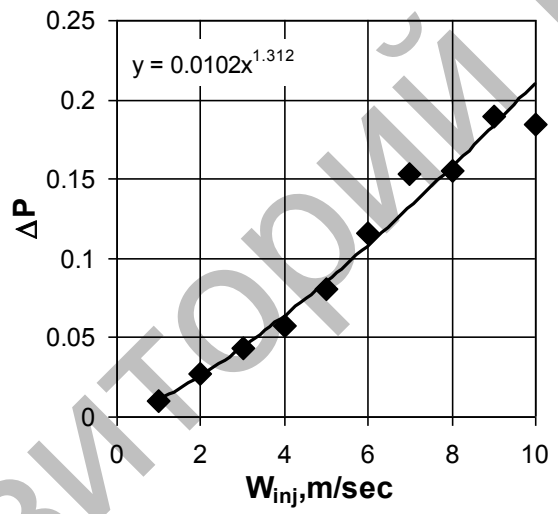

Fig. 9. Dependence of feed pressure on the injected water velocity

4 Ratio of flow rates at outlets

The split-parameter (S), which is defined as the ratio of water flows through both output openings of apparatus (overflow and underflow water) is of great importance to the separation process and can be given as follows:

$$S = \frac{Q_{ov}}{Q_{un}}$$

The fine particles are divided proportional to the ratio of water flows through these outlets. For conventional hydrocyclone (without injection), the split parameter increases if the feed pressure increases, as it is shown in Fig. 10. This trend is agreed with the investigations of Bradley [24] while it is contradicts to the work of Tarjan [25].

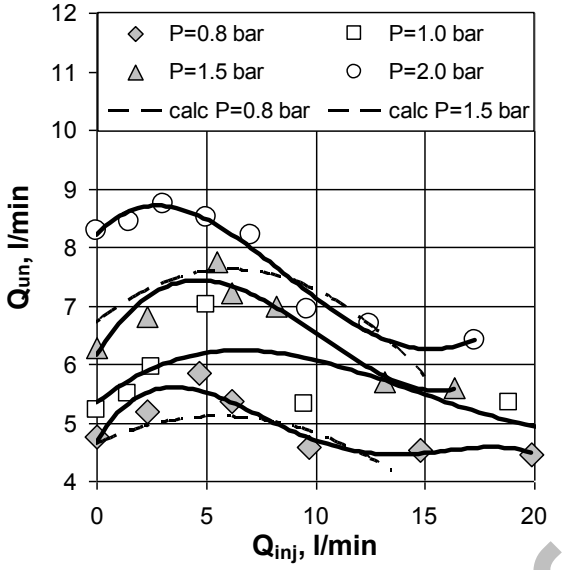

Fig. 10. The volumetric flow rate through the underflow discharge as dependent on the injection velocity. (Symbols and solid curves are the experimental data, dashed ones are the calculations)

Herewith, at constant feed pressure the effect of injection velocity on the split parameter (S) is investigated. Experiments have showed that the increase in injection velocity at low values (up to 5 lpm) leads to an increase in the fluid flow through the underflow, while at high velocity values it leads to decrease in the underflow throughput as seen in Fig. 10. The same trend was also obtained from the modeling calculations as shown in Fig. 10.

Fig. 11 shows the change of the split parameter related to throughput of the injected water (Q_{inj}) at different feed pressure values. From this figure, it can be seen that the estimated numerical values of the split parameter $S(Q_{inj})$ are agreed qualitatively well with the experimental data. The split parameter $S(Q_{inj})$ decreases gradually by increasing Q_{inj} in a small range. Further increase of Q_{inj} leads to gradually increase of the split-parameter $S(Q_{inj})$ values. So, it can be concluded that the trend of the split-parameter curve as a dependent on Q_{inj} is non monotone.

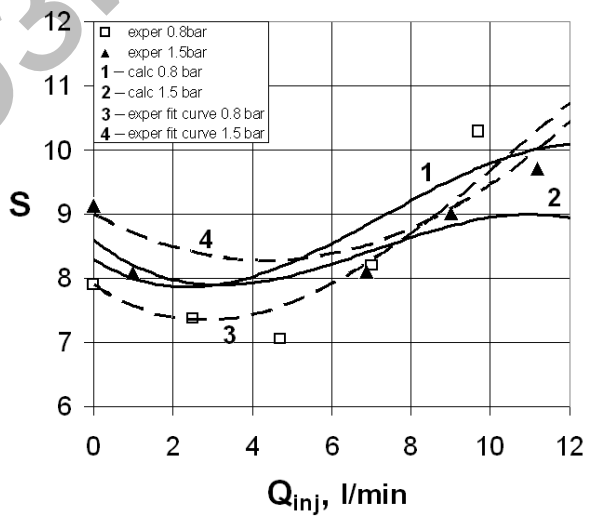

Fig. 11: Effect of the injection throughput on the split parameter

Discussion

Injection of water through the hydrocyclone may significantly change the hydrodynamic field in the apparatus. This change is particularly strong near the injection inlets. The present work examined the impact of tangential injection of water through the injector, located at the bottom of the conical part of the hydrocyclone. The influence of tangential injection is found to be the highest hydrodynamic impact on the classification process.

The calculation results have showed that the injection influence is not only due to the change of radial velocity component, as it was supposed, i.e. carrying out the particles from near the wall zone into the axis region and then to be separated in the overflow outlet. This can be shown apparently from Fig. 8, where the radial velocity changes its sign (radial speed changes its direction) at intervals along radial coordinate from the axis towards the wall.

The other reason which could be more possible to explain the injection effect is by considering the mechanism influencing the particles (if they would be in a flow), that is connected with the change of the axial component as follows:

A powerful stream of liquid arises upward during enough strong injection at the conical wall of the hydrocyclone, should move out the particles upwards specially the fines up to the cylindrical part of the cyclone. Some of these particles which follow the flow lines as it is shown in Fig. 5, will be directed to the overflow, another will return downwards again and be compelled to undergo again through the hydrodynamic influence of injector.

Apparently, that probability of such particles to be transported through the underflow discharge is much lower in comparison with similar probability for particles, which do not be influenced by injected jets.

This circumstance well proves to be true in experiments [16 – 21], where significant decrease of values of the separation function (analogue of discussed probability of carrying out the particles through the apex) for fine particles was observed.

Concerning the effect of the tangential velocity, the results have showed that the increase of injection throughput leads to a growth in the centrifugal force (tangential velocity component). This force affects on the particles and brings them out towards the hydrocyclone wall. It is known that the larger are the particles the higher is the effect. Thus for fine particles the increase in tangential velocity practically will not cause any effect, while the coarse particles should leave more effectively to a wall, and, finally, to apex.

The presented calculations show, that the influence of injection on the flow in the hydrocyclone is affected by alteration the velocity field by injected water. At low water injection rate, the injected tangential water slows the mean stream, especially its tangential component (Fig. 7), but at high injection speed, it accelerates the tangential component. This complex influence of injection affects dependence on the distribution of quantity of injected water between both outlets (overflow and underflow).

Experiments and calculations showed a non monotonous change of a portion of the injected water which goes through the underflow discharge. This explains the change of the influence mechanism of the injected water on the main flow.

Conclusions

The influence of tangential water injection through an injector, located at the conical part just above the apex, on the mean stream in a hydrocyclone is investigated. The injection of water in a hydrocyclone can markedly change the hydrodynamic fields in the device.

On the basis of the calculations partially supported by measurements, the explanation of the mechanism of influence of an injector on separation characteristics of a hydrocyclone is presented.

The mechanism is based on the generation of the axial streams which have been directed upwards that leads the recirculation of particles in the device and to lowering of value of probability for fine particles to be transported through the underflow discharge.

At low water injected rates, the mean stream is broken, but at high ones it is accelerated. It leads to non monotone dependence of a fraction of the injected water allocated through the underflow aperture.

References:

1. Pericleous, K.A., Rhodes, N., "The hydrocyclone classifier – a numerical approach," International Journal of Mineral Processing, **Vol. 56**, pp. 23-43, 1986.
2. M.R. Davidson, "Simularity solution for flow in hydrocyclones," Chem. Eng. Sci., 43 (7) pp. 1499-1505, 1988.
3. K. T. Hsien, R.K. Rajamani, "Mathematical model of the hydrocyclone based of fluid flow," AIChE J., 37 (5), pp.735-746, 1991.
4. Monredon, T.C., Hsien, K.T. and Rajamani, R.K., "Fluid flow model of the hydrocyclone: an investigation of device dimensions," International Journal of Mineral Processing, **Vol. 35**, pp. 65-83, 1992.
5. T.Dyakowski, R.A. Williams, "Modelling turbulent flow within a small-diameter hydrocyclone," Chem. Eng. Sci. 48 (6), pp. 1143-1152, 1993.
6. P. He, M. Salcudean, I.S. Gartshore, "A numerical simulation of hydrocyclones," Trans. Inst. Chem. Eng. J. Part A 7, pp. 429-441, 1999.
7. G. Q. Dai, J.M. Li, W.M. Chen, "Numerical prediction of the liquid flow within a hydrocyclone," Chem. Eng. J. 74, pp. 217-223, 1999.
8. Novakowski, A. F., Kraipech, W., Dyakowski, T., and Williams, R.A., "The hydrodynamics of a hydrocyclone based on a three-dimensional multi-continuum model," Chem. Eng. J., **Vol. 80**, pp. 275–282, 2000.
9. J. Ko , S. Zahrai, O. Macchion, H. Vomhoff , "Numerical modeling of highly swirling flows in a through-flow cylindrical hydrocyclone," AIChE Journal, 52, 10, pp. 3334 – 3344, 2006.
10. Nowakowski, J. C. Cullivan, R. A. Williams, and T. Dyakowski, "Application of CFD to modelling of the flow in hydrocyclones. Is this a realizable option or still a research challenge? ," Minerals Engineering. Vol. 17, Issue 5, pp. 661-669, May 2004.
11. Dueck, J., Matvienko, O.V., and Neesse, Th., "Modeling of Hydrodynamics and Separation in a Hydrocyclone," Theoretical Foundation of Chemical Engineering, Kluver Academic/Plenum Publishers, **Vol. 34**, No. 5, pp. 428-438, 2000.
12. Narasimha, M., Sripriya R., Banerjee, P. K., "CFD modelling of hydrocyclone- prediction of cut size," International Journal of Mineral Processing, **Vol. 75**, pp. 53-68, 2005.
13. S.Schütz, M. Piesche, G. Gorbach, M. Schiling, C. Seyfert, P. Kopf, T. Deuschle, N. Sautter, E. Popp, T. Warth, "CFD in der mechanischen Trenntechnik," Chemie Ingenieur Technik 79, 11, pp. 1777 – 1796, 2007.
14. Neesse, T. and Dueck, J., "Dynamic modelling of the hydrocyclone," .Minerals Engineering, **Vol. 20**, pp. 380-386, 2007.
15. Neesse, T. and Dueck, J., "CFD – basierte Modellierung der Hydrozyklonklassierung," Chemie Ingenieur Technik 79, 11, pp. 1931 – 1938, 2007.
16. Heiskanen, K., "Particle Classification," Chapman and Hall, London–Glasgow–New York–Tokyo–Melbourne–Madras, 321 pp., 1993.
17. D.D. Patil, T.C. Rao., Technical Note. "Classification evaluation of water injected hydrocyclone," Mineral Engineering, **Vol. 12**, no. 12, pp. 1527- 1532, 1999.
18. D.F. Kelsall, J.A. Holmes, "Improvement in classification efficiency in hydraulic cyclones by water injection," In. Proc. 5th Mineral processing Congress, Paper 9, Inst. Of Mining and Metallurgy, pp. 159-170, 1990.
19. R.Q. Honaker, A.V. Ozsever, N. Singh, B. K. Parekh, "Apex water Injection for improved hydrocyclone classification efficiency," Mineral Engineeering, , **Vol. 14**, No. 11, pp. 1445- 1457, 2001.
20. K. Udaya Bhaskar, B. Govindarajan, J.P. Barnawal, K.K. Rao, T.C. Rao, "Modelling studies on a 100 mm water-injection cyclone," Physical Separation in Science and Engineering, September-December, **Vol. 13**, no. 3-4, pp. 89 – 99, 2004.
21. K. Udaya Bhaskar, B. Govindarajan, J.P. Barnawal, K.K. Rao, B.K. Gupta, T.C. Rao, "Classification studies of lead-zinc ore fines using water-injection cyclone," Intern. Journ. Mineral Processing, 77 ,pp. 80-94, 2005
22. J.G. Dueck, E.V. Pikushchak, and L.L. Minkov, "Modelling of change of the classifiers separation characteristics by water injection into the apparatus," Thermophysics and Aeromechanics, **Vol. 16**, No. 2, pp. 247-258, 2009.
23. Yakhot, V., Orszag, S.A., Thangam, S., Gatski, T.B. & Speziale, C.G., "Development of turbulence models for shear flows by a double expansion technique," Physics of Fluids A , **Vol. 4**, No. 7, pp.1510-1520, 1992.
24. Bradley D., "The Hydrocyclone," Pergamon Press, London, 1965.
25. Tarjan, G., "Some theoretical questions on classifying and separating hydrocyclones," Acta tech. Acad. Sci., 32, pp. 357 – 388, 1961.